Precise comparison of the Gaussian expansion method and the Gamow shell model

H. Masui*
Information Processing Center, Kitami Institute of Technology, Kitami 090-8507, Japan

K. Katō
Nuclear Reaction Data Centre, Faculty of Science, Hokkaido University, Sapporo 060-0810, Japan

N. Michel
National Superconducting Cyclotron Laboratory, Department of Physics and Astronomy, Michigan State University, East Lansing, MI 48824 USA
Grand Accélérateur National d'Ions Lourds (GANIL), CEA/DSM – CNRS/IN2P3, BP 55027, F-14076 Caen Cedex, France

M. Płoszajczak
Grand Accélérateur National d'Ions Lourds (GANIL), CEA/DSM – CNRS/IN2P3, BP 55027, F-14076 Caen Cedex, France

(Dated: April 8, 2014)

We perform a detailed comparison of results of the Gamow Shell Model (GSM) and the Gaussian Expansion Method (GEM) supplemented by the complex scaling (CS) method for the same translationally-invariant cluster-orbital shell model (COSM) Hamiltonian. As a benchmark test, we calculate the ground state 0^+ and the first excited state 2^+ of mirror nuclei ^{6}He and ^{6}Be in the model space consisting of two valence nucleons in p-shell outside of a ^{4}He core. We find a good overall agreement of results obtained in these two different approaches, also for many-body resonances.

PACS numbers: 21.10.-k, 21.60.-n

arXiv:1403.0160v2 [nucl-th] 7 Apr 2014

I. INTRODUCTION

In recent years, the playground of nuclear physics has extended towards neutron and proton drip lines [1–3]. Huge amount of new experimental data on nuclei far from the valley of stability has been provided by new rare-isotope facilities. The knowledge of these nuclei has largely improved also due to the progress in theoretical methods and computing power which allows to calculate light nuclei in *ab initio* framework taking into account the proximity of the scattering continuum. The description of various manifestations of the continuum coupling requires the generalization of existing many-body methods and call for theories which unify structure and reactions.

Realistic studies of the coupling to continuum in the many-body framework can be made in the open quantum system extension of the Shell Model (SM), the so-called Continuum Shell Model (CSM) [4, 5]. A recent realization of the CSM is the complex-energy CSM based on the Berggren ensemble [6], the GSM, which finds a mathematical setting in the Rigged Hilbert Space [7]. This model is a natural generalization of the standard SM for the description of configuration mixing in weakly bound states and resonances. Berggren completeness relation can be derived from the Newton completeness relation [8] for the set of real-energy eigenstates by deforming the real momentum axis to include resonant poles which are located in the fourth quadrant of the complex k-plane. Thus the Berggren completeness relation which replaces the real-energy scattering states by the resonance contribution and a background of complex-energy continuum states, puts the resonance part of the spectrum on the same footing as the bound and scattering spectrum. As the benefit of the explicit inclusion of the non-resonant continuum and resonant poles, the contribution of the unbound states to the one- and two-body matrix elements can be discussed. Berggren ensemble has found the application in the GSM [9], time-dependent Green's function approach [10], the no-core GSM [11], the coupled cluster approach [12], the Density Matrix Renormalization Group (DMRG) approach [13], and in the coupled-channel GSM [14, 15] to study various nuclear structure and reaction problems.

Another approach is the complex scaling (CS) method [16], which has been used to solve many-body resonances in many fields including atomic physics, molecular physics [17, 18] and nuclear physics [19, 20]. In the CS method, asymptotically-divergent resonant states are described within $\mathcal{L}^2$-integrable functions through the rotation of space coordinates and their conjugate momenta in the complex plane. As basis functions, the Gaussian Expansion Method (GEM) [21] has been extensively employed for the cluster-orbital shell model (COSM) [22] and coupled rearrangement channel model such as the TV-model [23]. The CS-COSM has successfully been applied to description of resonant states observed above the many-body decay threshold in p-shell nuclei (A = 5-8) using a ^{4}He+XN model, where X = 1-

*Electronic address: hgmasui@mail.kitami-it.ac.jp

4 and $N = p$, n [24, 25]. The CS-TV model for the core+2N systems has been shown to reproduce the observed Coulomb breakup cross sections for three-body continuum energy states [26, 27].

The purpose of these studies is to perform a detailed comparison of the GSM and the GEM+CS results for ^{6}He and ^{6}Be using the same COSM coordinates for valence nucleons [22] and the same Hamiltonian. In COSM, all coordinates are taken with respect to the core Center-of-Mass (CoM), so that the translational invariance is strictly preserved. COSM combined with CS method has been employed in numerous studies of weakly bound states and resonances in light nuclei [23, 28–35]. COSM coordinates have been also used in GSM [36] to investigate isospin mixing in mirror nuclei [37] and charge radii in halo nuclei [38].

The paper is organized as follows. In Section II we present our COSM Hamiltonian and the model space. In Section III, the two theoretical approaches, namely the GEM+CS (Section III.A) and the GSM (Section III.B), are briefly introduced. GEM+CS and GSM results for ^{6}He and ^{6}Be are presented and discussed in Section IV. Finally, Section V gives the main conclusions of these studies.

II. THE COSM HAMILTONIAN

In these studies, we employ the three-body model for ^{4}He plus two-nucleon system in the COSM coordinates [22] (see Fig. 1).

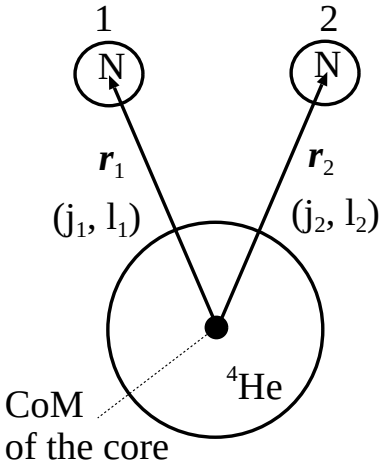

FIG. 1: Coordinate system of the COSM approach.

The Hamiltonian is written as follows:

$$\hat{H} = \sum_{i=1}^{2} \left(\hat{t}_i + \hat{V}_i^{(C)} \right) + \left(\hat{T}_{12} + \hat{v}_{12} + \hat{V}_{12}^{(C)} \right) \ , \qquad (1)$$

where $\hat{t}_i$ and $\hat{V}_i^{(C)}$ are the kinetic and potential energy operators for the ^{4}He core and an ith valence nucleon subsystem. In Eq. (1), the first parenthesis corresponds to the single-particle Hamiltonian for the ith valence nucleon, which is defined as

$$\hat{h}_i \ \equiv \ \hat{t}_i + \hat{V}_i^{(C)}, \ \ (i = 1, 2) \ . \qquad (2)$$

In the second parenthesis of Eq. (1), $\hat{v}_{12}$ is the nucleon-nucleon interaction for valence particles, and:

$$\hat{T}_{12} = -\frac{\hbar^2}{M^{(C)}} \nabla_1 \cdot \nabla_2 \ , \qquad (3)$$

is the recoil part which comes from the subtraction of the center of mass (CoM) motion, due to the finite mass $M^{(C)}$ of the core nucleus. The last term of Eq. (1) is the three-body potential of ^{4}He and two valence nucleons.

The interaction $\hat{V}_i^{(C)}$ between the core and the ith valence nucleon contains three terms:

$$\hat{V}_i^{(C)} = \hat{V}_i^{\alpha n} + \hat{V}_i^{\rm Coul} + \lambda \, \hat{\Lambda}_i \ , \quad (i = 1, 2) \ . \qquad (4)$$

The nuclear interaction part $\hat{V}_i^{\alpha n}$ is the modified KKNN potential [23, 39], which reproduces the α-N phase shifts in the low energy region. This potential contains a central and an LS parts as

$$\hat{V}_i^{\alpha n}(r_i) \ = \ V_0^{\alpha n}(r_i) + 2 V_{LS}^{\alpha n}(r_i) \, \boldsymbol{L} \cdot \boldsymbol{S}, \ \ (i = 1, 2) \ , \qquad (5)$$

where $\boldsymbol{r}_i$ is the relative coordinate between ^{4}He and the ith valence nucleon. The central part of Eq. (5) is written as:

$$V_0^{\alpha n}(r_i) \ = \ \sum_{k=1}^{5} [(-1)^{\ell_i}]_k \, V_k^0 \, \exp(-\rho_k^0 \, r_i^2) \ , \qquad (6)$$

where $[(-1)^{\ell_i}]_k$ is given by:

$$[(-1)^{\ell_i}]_k = \left\{ \begin{array}{ll} 1 & (k = 1, 2) \\ (-1)^{\ell_i} & (k = 3, 4, 5) \end{array} \right. \ . \qquad (7)$$

The LS part is:

$$V_{LS}^{\alpha n}(r_i) \ = \ \sum_{m=1}^{3} \, f_m^{LS} \, V_m^{LS} \, \exp(-\rho_m^{LS} \, r_i^2) \ , \qquad (8)$$

where the factor f_m^{LS} is:

$$f_m^{LS} = \left\{ \begin{array}{ll} 1 & (m = 1) \\ 1 - 0.3 \times (-1)^{\ell_i} & (m = 2, 3) \end{array} \right. \ . \qquad (9)$$

Parameters of the modified KKNN potential [23, 39] are shown in Table I.

For the Coulomb part $\hat{V}_i^{\rm Coul}$ in Eq. (4), we use a folded-type Coulomb interaction for the ^{4}He+p subsystem:

$$\hat{V}_i^{\rm Coul}(r_i) = \frac{2e^2}{r_i} \, {\rm Erf}(\alpha \, r_i) \ , \qquad (10)$$

where ${\rm Erf}(r)$ is the error function, and $\alpha = 0.828$ fm^{-1}.

TABLE I: Parameters of the modified KKNN potential [23, 39] used in this calculation.

$k=$	1	2	3	4	5
V_k^0 [MeV]	−96.3	77.0	34.0	−85.0	51.0
ρ_k^0 [fm^{-2}]	0.36	0.90	0.20	0.53	2.50
V_k^{LS} [MeV]	−8.4	−10.0	10.0	—	—
ρ_k^{LS} [fm^{-2}]	0.52	0.396	2.20	—	—

TABLE II: Parameters of the Minnesota potential [40].

k	1	2	3
V_k^{nn}[MeV]	200	−178	−91.85
ρ_k^{nn}[fm^{-2}]	1.487	0.639	0.465
$W_k^{(u)}$	$u/2$	$u/4$	$u/4$
$M_k^{(u)}$	$(2-u)/2$	$(2-u)/4$	$(2-u)/4$
$B_k^{(u)}$	0	$u/4$	$-u/4$
$H_k^{(u)}$	0	$(2-u)/4$	$-(2-u)/4$

To eliminate the spurious states in the relative motion between ^{4}He-core and the valence nucleon in CS, we use a projection operator [41]:

$$\hat{\Lambda}_i = \lambda |FS\rangle\langle FS| \ , \tag{11}$$

where the forbidden state in the ^{4}He+N case; $|FS\rangle = |0s_{1/2}\rangle$, is given by the harmonic oscillator function with the size parameter $b = 1.4$ fm.

In GSM, the forbidden state is eliminated from the set of the single-particle states, ϕ_i, as

$$\phi_i \Rightarrow (1 - \hat{\Lambda}_i)\phi_i \ . \tag{12}$$

We can confirm that the core-particle potential (4) with the parameters given in Table I, reproduces experimental energies and widths of $3/2^-_1$ and $1/2^-_1$ resonances in the ^{5}He(^{4}He+n) and ^{5}Li(^{4}He+p) systems.

For the two-body interaction $\hat{v_{12}}(\boldsymbol{r}_{12})$ of valence nucleons, where $\boldsymbol{r}_{12} \equiv \boldsymbol{r}_1 - \boldsymbol{r}_2$, we use the Minnesota potential [40]:

$$\begin{aligned}&\hat{v}_{12}(\boldsymbol{r}_{12}) \\ &= \sum_{k=1}^{3} V_k^0 \left(W_k^{(u)} - M_k^{(u)} P^\sigma P^\tau + B_k^{(u)} P^\sigma - H_k^{(u)} P^\tau\right) \\ &\qquad \times \exp(-\rho_k \boldsymbol{r}_{12}^2) \ .\end{aligned} \tag{13}$$

Parameters of this interaction are summarized in Table II, and the exchange parameter is taken as $u = 1.0$. The Coulomb interaction between valence protons is taken as an ordinary $1/r$-type functional form.

It was shown that the binding energy of ^{6}He cannot be reproduced using the reliable one- and two-body potentials for core-particle and particle-particle parts, respectively [23, 29]. The correct binding energy in a system ^{4}He+N+N is recovered by using a simple two-body Gaussian interaction, mimicking a physical three-body effect in the system [29] as:

$$\hat{V}_{12}^{(\mathrm{C})}(r_1, r_2) = V_{\alpha nn}^0 \exp(-\rho_{\alpha nn}(r_1^2 + r_2^2)) \tag{14}$$

with the parameters $V_{\alpha nn}^0 = -0.41$ MeV and $\rho_{\alpha nn} = 5.102 \times 10^{-3}$ fm^{-2}.

III. THE MODELS

In this section, we discuss two models for solving ^{4}He+2N (N is proton or neutron) systems with the COSM Hamiltonian. One is the GEM+CS approach, and another one is the GSM approach. The essential differences between the GEM+CS and GSM approaches are the choice of the basis functions and the treatment of continuum states.

The basis function $\Phi(\boldsymbol{r}_1, \boldsymbol{r}_2)$ in COSM is defined with a product of the functions with respect to each coordinate from the core to a valence nucleon,

$$\Phi(\boldsymbol{r}_1, \boldsymbol{r}_2)_{JM} \ \equiv \ [\mathcal{A}\{\phi_{\alpha_1}(\boldsymbol{r}_1) \otimes \phi_{\alpha_2}(\boldsymbol{r}_2)\}]_{JM} \ . \tag{15}$$

Here, α_i denotes the angular part of the ith particle $\{j_i, \ell_i\}$, and its z-components are implicitly included. $\mathcal{A}$ is the antisymmetrizer for particles 1 and 2.

The basis function for the ith valence nucleon is

$$\phi_{\alpha_i}(\boldsymbol{r}_i) = f(r_i)|j_i m_i\rangle \ . \tag{16}$$

The angular momentum part of the basis function is constructed by using the normal jj-coupling scheme as

$$|JM\rangle \ = \ |[j_1 \otimes j_2]_{JM}\rangle \ . \tag{17}$$

The above coupling procedure is the same both for GEM and GSM.

A. The Gaussian expansion method with complex scaling

The radial part of the GEM wave function is not an eigenfunction of the single-particle Hamiltonian $\hat{h}_i$, but the Gaussian function with the width parameter a as

$$\begin{aligned} f_{n_i}(r_i) \ &\equiv \ u_{\ell_1}^{n_i}(r_i) \\ &= \ N_i r_i^{\ell_i} \exp(-\frac{1}{2} a_{n_i} r_i^2) \ , \quad (i = 1, 2) \ , \end{aligned} \tag{18}$$

where N_i is the normalization, and ℓ_i is angular momentum for the ith nucleon.

The width parameter $a_{n_i} = 1/b_{n_i}^2$ in the GEM basis functions is defined using the geometric progression as: $b_{n_i} = b_0 \gamma^{n_i - 1}$ [21]. Here, b_0 and γ are input parameters, and n_i is an integer. The model space of the system is spanned by basis functions from $n_i = 1$ to $N_{\max}$. The kth eigenfunction $\psi_{k:\,\alpha_i}$ of the core+N system can be

obtained by diagonalizing the single-particle Hamiltonian $\hat{h}_i$ with the Gaussian basis functions,

$$\psi_{k:\,\alpha_i}(\boldsymbol{r}_i) = \sum_m^{N_{\max}} c_m^{(k)} \phi_{\alpha_i}^{(m)}(\boldsymbol{r}_i) \ . \tag{19}$$

Here, $\hat{h}_i \psi_{k:\,\alpha_i} = \epsilon_k \psi_{\alpha_i}$, and $c_m^{(k)}$ are determined by using the variational principle.

For solving the core+$2N$ system, the basis function (15) is given by the product of basis functions in Eq. (18) for particle 1 and 2 as follows:

$$\Phi_{JM}^{(m)} \ = \ \mathcal{A}\left\{ u_{\ell_1}^{(m)}(r_1) \cdot u_{\ell_2}^{(m)}(r_2) | JM \rangle^{(m)} \right\} \ . \tag{20}$$

Here, the width parameters $a_i^{(m)}$ in $u_{\ell_i}^{(m)}$ are prepared independently for particle 1 and 2. m is the index of the one-body basis functions.

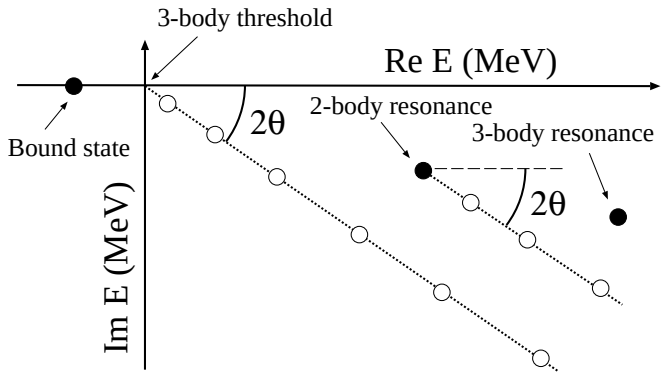

FIG. 2: Complex-scaled eigenstates of the three-body Hamiltonian for the Borromean system. Solid circles are bound and resonance states, and open circles are continuum states.

The calculation of two-body matrix elements (TBME), $\langle \Phi^{(m)} | \hat{O}_{12} | \Phi^{(n)} \rangle$ can be performed analytically. Even for different Gaussian width parameters, we can obtain the value of TBME without any approximations.

The solution of the core+$2N$ system can be obtained by diagonalizing the Hamiltonian

$$\hat{H} \Phi_{k:\,JM} = E_k \, \Phi_{k:\,JM} \ , \tag{21}$$

and the corresponding eigenfunction is expressed as a linear combination of the basis functions,

$$\Phi_{k:\,JM} \ = \ \sum_m^{N_{\rm Tot}} C_m^{(k)} \, \Phi_{JM}^{(m)} \ . \tag{22}$$

In order to treat the many-body resonant states, we apply the CS method. In this method, the coordinate and momentum are transformed using a rotation angle θ as:

$$r \to r\, e^{i\theta} \quad (k \to k\, e^{-i\theta}) \ . \tag{23}$$

Resonance wave functions, which diverge in the asymptotic region, can be converged with this transformation for a suitable rotation angle. This essential feature is proven by the ABC-Theorem [16, 42]. After this transformation, all continuum states are aligned along the rotated axis. Furthermore, using GEM, the continuum states are automatically discretized through the diagonalization of the Hamiltonian. A schematic figure of the bound states and resonances and discretized continuum states are shown for the Borromean system like ^{4}He+N+N in Fig. 2.

B. Gamow shell model approach

Another approach to study many-body resonances is the GSM approach [9, 11–13]. This generalization of the nuclear SM treats single-particle bound, resonance and continuum states on the same footing using a complete Berggren single-particle basis [6]:

$$\mathbf{1} \ = \ \sum_{i \in b,r} |\phi_i\rangle\langle\phi_i| + \oint_{\Gamma_k} dk |\phi(k)\rangle\langle\phi(k)| \ , \tag{24}$$

where Γ_k is a deformed momentum contour. For each (ℓ, j) of the resonant single-particle state in the basis, the set $(\ell, j)_{\rm c}$ of continuum states along the discretized contour in k-plane enclosing the resonant state(s) (ℓ, j) is included in the basis (see Fig. 3):

$$\mathbf{1} \ \simeq \ \sum_{i \in b,r} |\phi_i\rangle\langle\phi_i| + \sum_{\eta \in {\rm cont}} |\phi(k_\eta)\rangle\langle\phi(k_\eta)| \ , \tag{25}$$

where k_η are linear momenta discretized on the deformed contour with the parameters of a maximum k and a number of discretized points. Different shapes of (ℓ, j)-contours are equivalent unless the number of resonant states contained in them changes. The complete many-body basis is then formed by all Slater determinants where nucleons occupy the single-particle states of a complete Berggren ensemble [9].

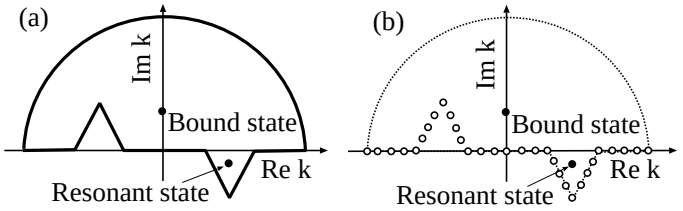

FIG. 3: Deformed contour on the complex momentum plane (a), and discretized continuum states along the deformed contour (b). Solid circles are bound and resonant states, and open circles are discretized continuum states.

In the Berggren basis, the basis function of the core+$2N$ system is:

$$\Phi_{JM}^{(\nu)} \ = \ \mathcal{A}\left\{ [\phi_1^{(\nu)} \otimes \phi_2^{(\nu)}]_{JM} \right\} \ . \tag{26}$$

Here, $\phi_i^{(\nu)}$ are single-particle bound, resonance, and discretized-continuum states for particles 1 and 2.

In GSM, the deformed contour for each (ℓ, j) is varied to obtain the best numerical precision of calculated eigenenergies and eigenvalues for a given discretization of the contour. Since the direct calculation of the TBME using the continuum and/or resonant single-particle states is numerically demanding, and even difficult to define from a theoretical point of view for some particular instances, one calculates TBME using the harmonic oscillator (HO) expansion procedure [36]. For the TBME between GSM basis functions $\Phi^{(i)}_{\rm GSM}$ and $\Phi^{(j)}_{\rm GSM}$, one obtains:

$$\begin{aligned}
&\langle\Phi^{(i)}_{\rm GSM}|\hat{O}_{12}|\Phi^{(j)}_{\rm GSM}\rangle \\
&= \sum_{\alpha,\beta}\langle\Phi^{(i)}_{\rm GSM}|\Phi^{(\alpha)}_{\rm HO}\rangle\langle\Phi^{(\alpha)}_{\rm HO}|\hat{O}_{12}|\Phi^{(\beta)}_{\rm HO}\rangle\langle\Phi^{(\beta)}_{\rm HO}|\Phi^{(j)}_{\rm GSM}\rangle \\
&= \sum_{\alpha,\beta} d^*_{i,\alpha}\, d_{j,\beta}\langle\Phi^{(\alpha)}_{\rm HO}|\hat{O}_{12}|\Phi^{(\beta)}_{\rm HO}\rangle\ , \qquad (27)
\end{aligned}$$

where $\Phi^{(\alpha)}_{\rm HO}$ are HO basis functions and $d_{i,\alpha}$ is the overlap between the GSM basis function $\Phi^{(i)}_{\rm GSM}$ and the HO basis function:

$$d_{i,\alpha} \equiv \langle\Phi^{(\beta)}_{\rm HO}|\Phi^{(i)}_{\rm GSM}\rangle\ . \qquad (28)$$

The advantage of this procedure is that the TBMEs with the HO expansion can be stored for a fixed $b_{\rm HO}$, and one only needs to calculate the overlaps $d_{i,\alpha}$, whatever the Berggren states are.

IV. RESULTS

For numerical calculations, we define the number of basis states. In the GEM+CS approach, the number of radial wave functions for each valence nucleon $N_{\rm max}$ is $N_{\rm max} = 22$. The typical value of the Gaussian width parameters are $b_0 = 0.1$ fm and $\gamma = 1.3$. Hence, the maximum size of the width parameter becomes $b = b_0\gamma^{N_{\rm max}-1} = 0.1 \times 1.3^{21} \simeq 25$ fm.

In GSM, the continuum is discretized with 40 points for each partial wave and the maximum momentum is $k_{\rm max} = 3.5$ fm^{-1}.

A. ^{6}He in the ^{4}He+2N model space

First, we show results for the ground state 0^+_1 and the first excited state 2^+_1 of ^{6}He. The ground state of ^{6}He is bound one with an energy $E = 0.97$ MeV from the ^{4}He+2n threshold. Hence, we can take the rotation angle as $\theta = 0$ for the calculation of this state in GEM+CS approach.

We calculate energies of ^{6}He by changing the maximum angular momentum for the coordinates $\boldsymbol{r}_1$ and $\boldsymbol{r}_2$ from $\ell_{\rm max} = 1$ to 5, where $\ell_{\rm max}$ is the maximum angular momentum in the basis function for the ^{4}He+n subsystem. Parameters of the interaction are chosen to reproduce the binding energy of the ground state of ^{6}He in a model space with $\ell_{\rm max} = 5$.

TABLE III: Energies of the ground 0^+_1 and the first excited 2^+_1 states of ^{6}He calculated using the GEM+CS and GSM approaches. All units except for the angular momentum are in MeV.

	$\ell_{\rm max}$	GEM+CS	GSM
$E(0^+_1)$	1	-0.117	-0.116
	2	-0.737	-0.737
	3	-0.870	-0.870
	4	-0.933	-0.932
	5	-0.978	-0.977
	$\ell_{\rm max}$	GEM+CS	GSM
$E(2^+_1)$	1	$0.805 - i0.086$	$0.804 - i0.086$
	2	$0.675 - i0.038$	$0.669 - i0.041$
	3	$0.628 - i0.027$	$0.619 - i0.030$
	4	$0.605 - i0.023$	$0.595 - i0.026$
	5	$0.589 - i0.021$	$0.577 - i0.024$

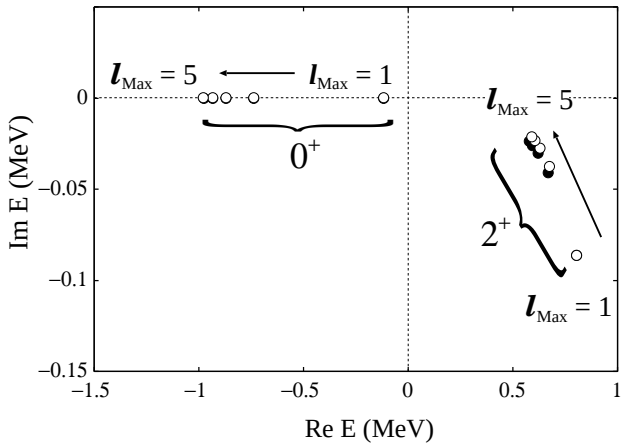

FIG. 4: Convergence of the poles of the ground 0^+_1 and the first excited 2^+_1 states of ^{6}He, which are calculated using the GEM+CS approach and the GSM for $1 \le \ell_{\rm max} \le 5$. Open and solid circles denote GEM+CS and GSM results, respectively.

The energies of the 0^+_1 state are shown in Table III for different values of $\ell_{\rm max}$. One can see that the calculation for $\ell_{\rm max} = 1$, which includes the $s_{1/2}$-, $p_{3/2}$- and $p_{1/2}$-orbits of the ^{4}He+N system, is not enough to reproduce the binding energy of ^{6}He. The inclusion of higher angular momenta ($\ell_{\rm max} \ge 2$) improves the calculated energy significantly. Nevertheless, even $\ell_{\rm max} = 5$ is not enough to obtain the converged ground state energy since the T-type Jaccobi configuration of valence neutrons is very important [23]. However, since the scope of this paper is to compare results of GEM+CS approach and GSM, we restrict the maximum angular momentum

for the core+N system to $\ell_{\max} = 5$ and determine the interaction parameters in this model space.

We find a good agreement between GEM+CS and GSM for a Borromean ^{6}He nucleus. The $\ell_{\max}$-dependence of the 0^+_1 and 2^+_1 energies is shown in Table III and Fig. 4.

The density of valence neutrons in the 0^+_1 state of ^{6}He is plotted in Fig. 5. One can see that the GEM+CS and GSM approaches give indistinguishable results for the density distributions in the 0^+_1 halo configuration of ^{6}He.

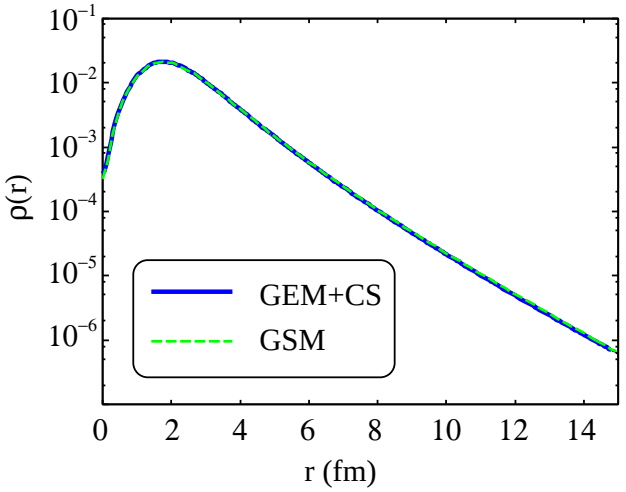

FIG. 5: (Color online) The density of valence neutrons in COSM coordinate system for the ground 0^+_1 state of ^{6}He (color online). The normalization of the density distribution is 1.

Results for the 2^+_1 narrow resonance are shown in Table III and Fig. 4. The difference between GEM+CS and GSM results in this case is at most ∼10 keV. The trajectories of the 2^+_1 state of the GEM+CS and GSM poles are shown in Fig. 4. Similarly, as for the 0^+_1-state, results of the GEM+CS and GSM approaches agree well.

B. ^{6}Be in the ^{4}He+2N model space

The ^{6}Be nucleus, the mirror system of ^{6}He, is unbound in the ground state. In this section, we shall compare results of GEM+CS and GSM for the 0^+_1 and 2^+_1 states of ^{6}Be described as a ^{4}He+2p three-body system.

Calculated energies of the 0^+_1 and 2^+_1 states for different $\ell_{\max}$ values are shown in Table IV. The difference of GEM+CS and GSM energies is less than ∼10 keV for the 0^+_1 state and ∼20 keV for the 2^+_1 state.

The trajectory of the 0^+_1 and 2^+_1 poles in the complex energy plane is shown in Fig. 6. Contrary to the 0^+_1 state, one may notice a slight difference between trajectories of 2^+_1-poles in GEM+CS approach and in GSM. This difference diminishes with increasing $\ell_{\max}$.

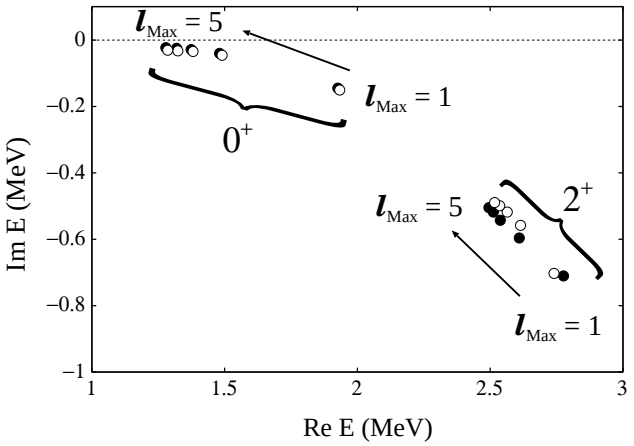

FIG. 6: Poles of the ground and first excited states of ^{6}Be calculated using GEM+CS approach and GSM from $\ell_{\max} = 1$ to 5. Open and solid circles correspond to GEM+CS and GSM results, respectively.

TABLE IV: Energies of the ground 0^+_1 and the first excited 2^+_1 states of ^{6}Be calculated using the GEM+CS and GSM approaches. All units except for the angular momentum are in MeV.

	$\ell_{\max}$	GEM+CS	GSM
	1	$1.932 - i0.152$	$1.926 - i0.146$
	2	$1.490 - i0.046$	$1.482 - i0.041$
$E(0^+_1)$	3	$1.380 - i0.036$	$1.374 - i0.030$
	4	$1.324 - i0.033$	$1.318 - i0.026$
	5	$1.285 - i0.031$	$1.279 - i0.024$
	$\ell_{\max}$	GEM+CS	GSM
	1	$2.741 - i0.703$	$2.776 - i0.711$
	2	$2.614 - i0.559$	$2.610 - i0.596$
$E(2^+_1)$	3	$2.565 - i0.518$	$2.538 - i0.543$
	4	$2.537 - i0.500$	$2.512 - i0.518$
	5	$2.517 - i0.491$	$2.495 - i0.505$

C. Discussion

In the comparison between the GEM+CS and GSM approaches, we obtain a good agreement for the bound state 0^+_1 in ^{6}He, and narrow resonances; 2^+_1 in ^{6}He and 0^+_1 in ^{6}Be. A small difference appears only for the 2^+_1 broad resonance in ^{6}Be. Below, we shall discuss a possible origin of such a small difference in the numerical results.

Both GEM+CS and GSM approaches solve the non-Hermitian problem. In the GEM+CS approach, the wave function of a resonance becomes $\mathcal{L}^2$-integrable with the help of the complex rotation. As a result, the Hamiltonian becomes non-Hermitian. The standard procedure to find the optimum values of the parameters is to search for a stationary point of the eigenvalue with respect to the variational parameters. The variational parameters are the complex rotation angle θ and the parameter b_0 in a definition of the Gaussian width; $b_{n_i} = b_0\gamma^{n_i-1}$ [31] for

the Gaussian basis functions. The optimization procedure is a simplified version of the generalized variational principle for complex eigenvalues [43]. The procedure works efficiently and gives very accurate solutions even for broad resonant states [31].

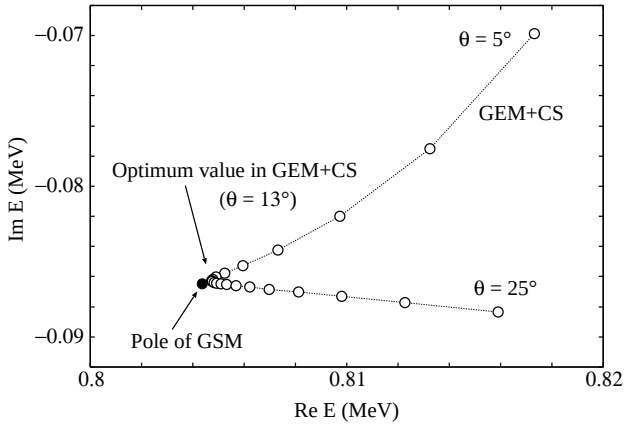

FIG. 7: Poles of ^{6}He (2^+) with $\ell_{\max} = 1$. For GEM+CS, we change the rotation angle θ from 5° to 25° in step of 1°.

GSM is formulated in the Berggren set, which includes bound single-particle states, single-particle resonances and scattering states from the discretized contour for each considered (ℓ, j). Consequently, the Hamiltonian matrix in this basis becomes complex-symmetric. The number of scattering states on each discretized contour (ℓ, j) and the momentum cutoff have to be chosen to assure the completeness of many-body calculations. Moreover, in the HO expansion procedure of calculating the TBMEs, the dependence on the oscillator length and the number of oscillator shells should be carefully examined.

Fig. 7 presents a trajectory of the 2^+_1 narrow resonant pole of ^{6}He calculated in the GEM+CS approach by changing the rotation angle θ, where the stationary point at the optimum value of the rotation angle is $\theta_{\rm opt} = 13°$, and the optimum point for the GSM calculation, which is obtained with the oscillator length and the number of oscillator shells are $b_{\rm HO} = 2$ fm and $N = 41$, respectively. In this case, the difference is only ~ 1 keV, and both methods give almost the equivalent result.

On the other hand, the 2^+_1 state of ^{6}Be is a broad resonant pole due to the presence of the Coulomb force for all three particles. The optimum value of the rotation angle in GEM+CS calculation is $\theta_{\rm opt} = 17°$, and the optimal HO oscillator length in GSM calculations is $b_{\rm HO} = 3$ fm. The difference of complex GEM+CS and GSM eigenenergies becomes in the order of 10 keV. To improve the agreement for the eigenvalues obtained by GEM+CS and GSM, it would be necessary to examine the optimization of the variational parameters more precisely. However, in the practical point of view, the difference is only less than 1 percent to the total energy.

The convergence can be tested by introducing an extrapolation procedure, e.g. the Richardson extrapolation [44]. We extrapolate the energy E as a function of $1/\ell_{\max}$ to $1/\ell_{\max} = 0$. The energies $E(1/\ell_{\max})$ of the 2^+-state of ^{6}Be become $2.483 - i0.474$ and $2.464 - i0.481$ (MeV) for GSM+CS and GSM, respectively. The difference becomes smaller than that of the $\ell_{\max} = 5$ case. Hence, we can conclude that both methods provide a sufficient accuracy even for the calculation of the broad resonant states.

V. SUMMARY

GSM and GEM+CS are two different theoretical approaches which allow to describe unbound resonant states. These two approaches differ in the choice of the basis functions and the numerical procedure to obtain the eigenvalues. To benchmark GSM and GEM+CS approaches, we have performed a precise comparison for weakly bound and unbound states using the same Hamiltonian in the COSM coordinates preserving the translational invariance. For a weakly bound ground-state of ^{6}He, GSM and GEM+CS give essentially identical results. For the three-body resonance states, GEM+CS and GSM give very close results proving the reliability of both schemes of the calculation for unbound states. The slight difference between GSM and GEM+CS results for broad resonances may have different origins. The HO expansion procedure in calculating the TBMEs in GSM may lead to rounding errors, especially for broad many-body resonances. On the other hand, the stationarity condition in GEM+CS approach could also be a source of small imprecision for broad resonances. Based on our results, we conclude that both approaches are essentially equivalent for all quantities studied. The other work for a comparison in the ^{6}He system has been done and also shows a good agreement between two different approaches [45].

Acknowledgments

We would like to thank W. Nazarewicz and members of the nuclear theory group at Hokkaido University for fruitful discussions. This work was supported by the Grant-in-Aid for Scientific Research (No. 21740154) from the Japan Society for the Promotion of Science, and FUSTIPEN (French-U.S. Theory Institute for Physics with Exotic Nuclei) under DOE grant number DE-FG02-10ER41700.

[1] I. Tanihata *et al.*, Phys. Rev. Lett. **55**, 2676 (1985).

[2] A. Ozawa *et al.*, Nucl. Phys. **A691**, 599 (2001).

[3] A. Ozawa, T. Suzuki, and I. Tanihata, Nucl. Phys. **A693**, 32 (2001).

[4] J. Okołowicz, M. Płoszajczak, and I. Rotter, Phys. Rep. **374**, 271 (2003).

[5] A. Volya, and V. Zelevinsky, Phys. Rev. C **74**, 064314 (2006).

[6] T. Berggren, Nucl. Phys. **A109**, 265 (1968).

[7] I.M. Gel'fand and N.Ya. Vilenkin, *Generalized Functions*, Vol. 4, Academic Press, New York (1961);
K. Maurin, *Generalized Eigenfunction Expansions and Unitary Representations of Topological Groups*, Polish Scientific Publishers, Warsaw (1968);
A. Bohm, *The Rigged Hilbert Space and Quantum Mechanics*, Lecture Notes in Physics 78, Springer, New York (1978).

[8] R. Newton, J. Math. Phys. **1**, 319 (1960).

[9] N. Michel, W. Nazarewicz, M. Płoszajczak and K. Bennaceur, Phys. Rev. Lett. **89**, 042502 (2002);
R. Id Betan, R. J. Liotta, N. Sandulescu and T. Vertse, Phys. Rev. Lett. **89**, 042501 (2002);
N. Michel, W. Nazarewicz, M. Płoszajczak and J. Okołowicz, Phys. Rev. C **67**, 054311 (2003);
N. Michel, W. Nazarewicz and M. Płoszajczak, Phys. Rev. C **70**, 064313 (2004).

[10] A. Volya, Phys. Rev. C **79**, 044308 (2009).

[11] G. Papadimitriou, J. Rotureau, N. Michel, M. Płoszajczak and B.R. Barrett, arXiv:1301.7140.

[12] G. Hagen, D. J. Dean, M. Hjorth-Jensen and T. Papenbrock, Phys. Lett. **B656**, 169 (2007).

[13] J. Rotureau, N. Michel, W. Nazarewicz, M. Ploszajczak and J. Dukelsky, Phys. Rev. Lett. **97**, 110603 (2006).

[14] Y.Jaganathen, N.Michel and M.Płoszajczak, Journal of Physics: Conference Series **403**, 012022 (2012).

[15] R.M. Id Betan, Phys. Lett. **B730**, 18 (2014).

[16] J. Aguilar and J. M. Combes, Commun. Math. Phys. **22**, 269 (1971).

[17] Y.K. Ho, Phys. Rep. **99**, 1 (1983).

[18] N. Moiseyev, Phys. Rep. **302**, 211 (1998).

[19] B. Gyarmati and A. T. Kruppa, Phys. Rev. C **34**, 95 (1986).

[20] S. Aoyama, T. Myo, K. Katō and K. Ikeda, Prog. Theor. Phys. **116**, 1 (2006).

[21] E. Hiyama, Y. Kino and M. Kamimura, Prog. Part. Nucl. Phys. **51**, 223 (2003).

[22] Y. Suzuki and K. Ikeda, Phys. Rev. C **38**, 410 (1988).

[23] S. Aoyama, S. Mukai K. Katō and K. Ikeda, Prog. Theor. Phys. **93**, 99 (1995).

[24] T. Myo, R. Ando, K. Katō, Phys. Letters B **691**, (2010) 150.

[25] T. Myo, Y. Kikuchi, and Kiyoshi Katō, Phys. Rev. C **84**, 064306 (2011) and **85**, 034338 (2012)

[26] Y. Kikuchi, K. Katō, T. Myo, M. Takashina and K. Ikeda, Phys. Rev. C **81**, 044308 (2010).

[27] Y. Kikuchi, T. Myo, K. Katō and K. Ikeda, Phys. Rev. C **87**, 034606 (2013).

[28] T. Myo, A. Ohnishi and K. Katō, Prog. Theor. Phys. **99**, 801 (1998).

[29] T. Myo, K. Katō, S. Aoyama and K. Ikeda, Phys. Rev. C **63**, 054313 (2001).

[30] T. Myo, S. Aoyama, K. Katō and K. Ikeda, Prog. Theor. Phys. **108**, 133 (2002).

[31] S. Aoyama, T. Myo, K. Katō and K. Ikeda, Prog. Theor. Phys. **116**, 1 (2006).

[32] H. Masui, K. Katō and K. Ikeda, Phys. Rev. **C73**, 034318 (2006).

[33] H. Masui, K. Katō and K. Ikeda, Phys. Rev. **C75**, 034316 (2007).

[34] H. Masui, K. Katō and K. Ikeda, Eur. Phys. Jour. **A42**, 535 (2009).

[35] H. Masui, K. Katō and K. Ikeda, Nucl. Phys. **A895**, 1 (2012).

[36] N. Michel, W. Nazarewicz, M. Płoszajczak and T. Vertse, J. Phys. G: Nucl. Part. Phys. **36**, 013101 (2008).

[37] N. Michel, W. Nazarewicz and M. Płoszajczak, Phys. Rev. C **82**, 044315 (2010).

[38] G. Papadimitriou, A.T. Kruppa, N. Michel, W. Nazarewicz, M. Płoszajczak and J. Rotureau, Phys. Rev. C **84** 051304(R) (2011).

[39] H. Kanada, T. Kaneko, S. Nagata and M. Nomoto, Prog. Theor. Phys. **61**, 1327 (1979).

[40] D. R. Thompson, M. LeMere, and Y. C. Tang, Nucl. Phys. **A286**, 53 (1977).

[41] S. Saito, Prog. Theor. Phys. Suppl. **62**, 11 (1977).

[42] E. Balslev and J. M. Combes, Commun. Math. Phys. **22**, 280 (1971).

[43] N. Moiseyev, P.R. Certain, and F. Weinhold, Mol. Phys. **36**, 1613 (1978);
N. Moiseyev, Phys. Rep. **302**, 212 (1998).

[44] L. F. Richardson, Phil. Trans. R. Soc. Lond. A **210**, 307 (1911);
L. F. Richardson and J. A. Gaunt, Phil. Trans. R. Soc. Lond. A **226**, 299 (1927).

[45] A.T. Kruppa, G. Papadimitriou, W. Nazarewicz and N. Michel, Phys. Rev. C **89**, 014330 (2014).